Sciencia Acta Xaveriana
An International Science Journal
ISSN. 0976-1152

Volume 3
No. 1
pp. 45-60
Apr 2012

Third order nonlinear optical properties of 4-N, N-dimethylamino-4'-N'-methyl-stilbazolium iodide (DMSI) single crystal

R. Gunaseelan[1] S. Selvakumar[2] and P. Sagayaraj[1*]

[1] Dept.of Physics, Loyola College, Chennai- 600034, Inia

[2] Department of Physics, Nandanam Govt. Arts College, Chennai- 600 039, India

[1*] Associate professor of Physics, Loyola College, Chennai - 600 034, India
Email: psagayaraj@hotmail.com, Tel: +9144 28178200; Fax: +9144 28175566

Abstract : An organic single crystal 4-N,N-dimethylamino-4'-N'-methyl-stilbazolium iodide (DMSI) which has high third order optical nonlinearity was successfully grown by slow solvent evaporation technique at room temperature. The grown single crystal was subjected to different characterization analyses to find out its suitability for device fabrication. The single crystal X-ray diffraction (XRD) and powder XRD analyses confirmed the crystal structure. This compound was characterized by functional groups analyses using CHN and proton NMR spectrum. It is evident from the optical absorption study that the crystal has excellent transmission in the entire visible region with its lower cut off wavelength is around 572 nm. The thermal stability of the compound was determined by thermal analyses of the specimen. The electrical properties of the crystal are investigated by ac, dc and photoconductivity measurements.

Key words : Organic crystal; XRD; UV-Vis Absorption; TGA; Conductivity.

1. Introduction

A wide variety of materials have been investigated for third-order nonlinear optics, among which organic materials are advantageous because of their optical and electronic properties which can be tuned and tailored by structural modification [1]. Organic materials exhibiting strong nonlinear optical (NLO) properties one order magnitude higher than those of inorganic materials have attracted considerable interest because of their possible applications in opto-electronic and all-optical devices such as optical limiters optical switches and optical modulators [2, 3]. In recent years, π-conjugated organic compounds have been investigated as a new class of third-order NLO materials due to their high NLO properties and fast response time. The NLO behavior of organic molecules originates mainly from a strong donor–acceptor intermolecular interaction and delocalized p-electron system. Of the several organic compounds known to exhibit NLO properties, 4'-N- N-dimethylamino-4'-N'- methyl-stilbazolium iodide (DMSI) is known to have a high third order optical nonlinearity [4, 5] and ultrafast response due to the existence of delocalized π-electrons [4-7]. Nakamura et al have incorporated DMSI into SiO_2 gel and found that the third nonlinear susceptibility $\chi^{(3)}$ values of this dye doped gel to be twice as large as SiO_2 glass [5]. Single crystals are among the most attractive material because of their typically large macroscopic nonlinearities, high packing densities, and superior long–term orientational and photochemical stabilities as well as their optical quality compared to poled polymers [8, 9]. Developing DMSI in single crystalline form would enhance third nonlinear susceptibility $\chi^{(3)}$. The molecular structure of DMSI is shown in Fig. 1. Therefore we have investigated the growth of DMSI crystal by employing slow evaporation technique. The grown crystal was characterized by single crystal XRD, Powder XRD, NMR, UV-Vis absorption, TGA/DSC and impedance spectral analyses.

2. Experimental

2.1. Material Synthesis

DMSI was synthesized by the condensation of 1,4-dimethyl pyridinium iodide (2.35 g,10 mmol), methanol (30 ml) and 4-N, N-dimethylamino-benzaldehyde (1.79 g, 10 mmol) in the presence of piperidine (0.2 ml) [10]. The above mixture was refluxed for 12 hours and cooled to room temperature. The product was filtered and recrystallized from methanol at least three times.

2.2. Solubility measurement

The solubility of DMSI in methanol (solvent) was determined by adding a solute in solvent till it is completely dissolved. After attaining the saturation, the equilibrium concentration of the solute was analyzed gravimetrically. Using this technique, the solubility of DMSI at six different temperatures (30, 35, 40, 45, 50 and 55 ^{o}C) has been evaluated. The temperature dependence of solubility of DMSI is shown in Fig. 2. From the graph it is found that the solubility of DMSI increases with temperature.

2.3. Crystal Growth

Crystal growth was performed by employing slow evaporation technique. A saturated solution was prepared with 1.0 g of DMSI dissolved in 100 ml of methanol at 40^{o}C and then stirred for 1 hr. The beaker was sealed with a perforated lid and the solvent was allowed to evaporate slowly. As glass beakers produced only very poor needle crystals due to multi-nucleation, Teflon beaker was used in order to prevent the sticking of material to the side walls of the beaker during evaporation process. After 21days, crystals size of 9 x 5 x 3 mm^{3} was obtained (Fig. 3).

3. Results and discussion

3.1. Single crystal XRD

Single crystal X-ray diffraction data were collected by using ENRAF NONIUS CAD4-F single crystal X-ray diffractometer with MoKα (λ = 0.71073 Å) radiation. The structure was solved by the direct method and refined by the full matrix least square technique using the SHELXL program. It is observed that the grown crystal belongs to Monoclinic system with space group *P*21/*c*. The single crystal XRD data of the present work is confirms the structure of the grown crystal (Fig. 4- Ortep diagram). Table 1 presents the single crystal XRD data of DMSI sample. The results obtained for the crystals grown in the present work are in good agreement with the literature [11] and thus confirms the identity of DMSI.

3.2. Powder XRD study

Powder X-ray diffraction analysis (PXRD) was carried out using an X-ray diffractometer, MODEL RICH SEIFERT, XRD 3000P with monochromatic nickel filtered CuK_{α} (λ = 0.15406

nm) radiation. The sample was scanned over the range 10 - 55° at the rate of one degree/ minute. The input voltage and current were 35 kV and 30 mA respectively, and the slit width was 0.1 mm. The recorded powder X-ray diffraction pattern of DMSI is shown in Fig. 5. From the powder XRD data, the (h k l) and lattice parameter values of DMSI were calculated. The lattice parameters of DMSI are a = 6.3042 Å, b = 7.672 Å and c = 32.012 Å and V=1544.54 $Å^3$. The differences in the peak amplitudes can be attributed to the different sizes and orientations of the powdered grains. The results obtained from the powder XRD for the crystals grown in the present work are in good agreement with the single crystal XRD data.

3.3. CHN Analysis

The elemental composition of DMSI crystal was carried out by Perkin-Elmer 2400 Series CHNS/O analyzer and the experimental result of the elemental percentage is well coincide with the calculated values (Table 2).

3.4. NMR Spectrum study

The proton NMR spectrum was recorded using Burker AVANCE III 500 MHz FT NMR spectrometer. The proton NMR spectrum (Fig. 6) of DMSI was recorded by dissolving the sample in deuterated methanol. In the proton NMR spectrum of DMSI, the singlets at 3.088 and 4.233 are assigned to six hydrogens of N–$(CH_3)_2$ and three hydrogens of N–CH_3 respectively. The singlet at 4.868 is due to two hydrogens of NH_2 in the anion. The doublets at 6.801 and 7.62 are due to the four hydrogens of the N-$(CH_3)_2$-C_6H_4 aromatic ring. The doublets at 7.985 and 8.523 are due to the four hydrogens of the C_5H_4N aromatic ring. The doublets at 7.122 and 7.867 are due to the two oliphinic hydrogens (HC=CH). The multiplet observed at 3.33 is due to the solvent (CD_3OD).

3.5. UV-Vis-NIR absorption analysis

The absorption spectrum was recorded by a SHIMADZU model UV-2450 double-beam spectrophotometer in the wavelength range 200–1000 nm in solution form using methanol as solvent. Absence of absorption in the region between 572 and 1000 nm is an advantage as it is the key requirement for materials having NLO properties [12]. The spectrum gives two peaks, one intense peak at 478nm corresponding to $\pi - \pi^*$ transition and another at 272 nm

corresponds to n - π* transition (Fig. 7). Two optical band gaps were calculated for these transitions. The band gap corresponds to π – π* is 4.986 eV and for n - π* is 10.563 eV.

3.6. Thermal analysis

Thermal analysis (TG & DTG) was carried out using TGA Q500 V20.10 BUILD 36 N_2 atmosphere at the heating rate of 20 °C/min (Fig. 8a).

The DMSI compound undergoes decomposition by two stages. The first stage is the dehydration occurred between 30-100 °C (or below 100 °C). The 4 % weight loss occurred below 100 °C is due to the contaminated water molecule associated with the compound. The maximum weight loss, 80 % occurred in the range 200-340 °C. The compound undergoes decomposition and it is completely converted to gaseous products. DTG curve gives a peak temperature of 261.37 °C which is the sublimation temperature of DMSI.

DSC analysis of DMSI compound was carried out using DSC Q200 V24.4 BUILD 116, N_2 atmosphere at the heating rate of 10 °C/min on the temperature range of 30-290 °C (Fig. 8b). The spectrum indicates only one endothermic peak at 261.37 °C. The sharp endothermic point represents the sublimation energy which was found to be 12.873 kJ mol^{-1}.

3.7. Impedance spectral analysis

The *ac* conductivity study using complex impedance spectroscopy was performed on the DMSI crystal using HB 4124 LCR meter. The crystalline sample was powdered and pelletized into a rectangular slab of area 35 mm^2 and thickness 1 mm [13]. The ac conductivity study using complex impedance spectroscopy is performed to characterize the bulk resistance of the crystalline material [14]. In the present case, the complex impedance parameters are measured with HB 4124 LCR meter using silver electrodes. The crystalline sample was cut into a rectangular slab of area 40 mm^2 and thickness 1 mm. The sample was polished and silver coated to establish the ohmic contact. The ac conductivity of the sample is determined from the real part of the impedance using the relation

$$\sigma_{ac} = t/R_b A$$

Where t is the thickness, A is the area of face in contact with the electrode and R_b is the bulk resistance. The bulk resistance was found to be 2.486 x 10^5 Ω. The calculated ac conductivity

was 10.056 x 10^{-7} $(\Omega cm)^{-1}$. The plot of Z' and Z? for DMSI crystal at room temperature is shown in Fig. 9 and the obtained impedance exhibits a good semicircle. The observed value is typical for an insulating material. Interestingly, the observed low ac conductivity suggests that the number of defects or impurities present in the slow evaporation grown DMSI crystal is low.

3.8. Microhardness Studies

Vickers hardness indentations were made on the flat polished face of the crystal at room temperature for loads 10, 20, 30, 40, 50, 60, 70 and 80 g using Vickers hardness tester fitted with Vickers diamond intender and attached to an incident light microscope [15]. Crack initiation and material chipping became significant beyond 100 g of the applied load and hardness test thus could not be carried out further. The lengths of the two diagonals of the indentations were measured and the Vickers hardness number was computed using the formula $Hv = 1.8544\ p/d^2$, where Hv is the Vickers hardness number in kg/mm^2, p is the intender load in kg and d is the diagonal length of the impression in mm. A graph was plotted for hardness versus load (Fig. 10a) and log p versus log d (Fig. 10b). The plot of log p versus log d yields a straight line, and its slope gives the work hardening coefficient or the Meyers index number '*n*'. The value of *n* is found to be 2.809 and since the value of *n* is greater than 2, the hardness of the material is found to increase with the increase of load (Fig. 10b) which confirms the prediction of Onitsch [16] and also the reverse indentation size effect [17, 18]. From the Meyer's index number it is clear that the title material belongs to soft material category [15].

4. Conclusion

The development of nearly flat DMSI crystals requires thorough investigation on the growth procedures. Employing rapid evaporation of the DMSI-methanol solution with slow solvent evaporation method, thin needle of DMSI crystal of dimension 9 x 5 x 3 mm^3 are harvested in a period of 21 days. Our preliminary study indicates that through proper optimization of growth conditions such as concentration of the solution, temperature and growth rate, it is possible to grow good quality needle of DMSI by a simple and cost effective method. The grown crystal was characterized by XRD, CHN, and UV-Vis absorption studies. The microhardness test shows that the hardness value increases with load, which confirms the reverse indentation size effects of the crystal. The ac conductivity study of the sample have

been carried out. Owing to its transparency and centrosymmetric crystal structure, DMSI can be used as promising material for third order NLO applications.

Acknowledgement

The authors acknowledge the University Grants Commission (UGC), India for funding this research work (Ref. No. F. 38-119/2009(SR)).

References

[1] K. Kubodera and T. Kaino, Nonlinear Optics of Organic and Semiconductors, ed T. Kobayashi, (Springer, Berlin, 1989) p 163.

[2] D. Udayakumar , A. John Kiran , A. Vasudeva Adhikari, Chem. Phy. 331 (2006) 125–130.

[3] T. Taima ,K. Komatsu , T. Kaino , C.P. Franceschina , L. Tartara, Opt. Mater. 21 (2002) 83–86.

[4] Seetharam Shettigar and P.Poornesh , Opt. Laser Technol. 42 (2010) 1162– 1166.

[5] Maki Nakamura, Hiroyuki Nasu and Kanichi Kamiya, J. Non-Cryst. Solid 135 (1991) 1-7.

[6] T. Hayashi, New Glass (4) (1989) 34.

[7] T. Kobayashi, in Hikarijouhouairyou and Zairyoukougakuhen (Materials for Optical Communications), ed T Kamiya (Maruzen, Tokyo, 1988) p.183.

[8] G.R. Meredith, In nonlinear optical properties of Organic and Polymers Materials, Williams. D.J., Ed.; ACS Symposium Series Vol. 233; American Chem. Soc. Washington, DC, 1983: 27-56.

[9] B.B. Coe, J.A. Harris, I. Asselberghs, K. Wostyn, K. Clays, A. Persons, B.S. Brunsehwig, S.J. Coles, T. Gelbrich, M.I. Light, M.B. Huarthouse and K. Nakatani, Adv. Funct. Mater. 13 (2003) 347.

[10] H. Adachi, Y. Takahashi, J. Yabuzaki, Y. Mori and T. Sasaki, J. Cryst. Growth 198/199 (1999) 568.

[11] T.J. Lee, C. Wong and K.T. Kwo, J. Chin. Chem. Soc. (Taipei), 26 (1979) 53.

[12] X.M. Duan, S. Okada, H. Oikawa, H. Matsuda, H. Nakanishi, Jpn. J.Appl. Phys. 33 (1994) 1559.

[13] E. Barsoukov J.R. Macdonald, Impedance Spectroscopy Theory, Experiment, and Applications, 2nd Edition, John Wiley & Sons, New Jersey, 2005.

[14] R.P. Suvarna, K.R. Rao and K. Subbarangaiah, Bull. Mater. Sci. 25 (2002) 647.

[15] S.Kalainathan, K. Jagannathan, J. Cryst. Growth 310 (2008) 2043.

[16] E. M. Onitsch, Mikroskopie, 95 (1950) 12.

[17] K. Sangwal, Mater. Chem. Phys. 63 (2000) 145.

[18] P. V. Raja Shekar, D. Nagaraju, V. Ganesh, K. Kishan rao, Cryst. Res. Technol.44 (2009) 652.

Figure Caption

Fig. 1 Molecular structure of DMSI

Fig. 2 Solubility curve of DMSI

Fig. 3 Photograph of DMSI crystals

Fig. 4 Ortep diagram of DMSI single crystal

Fig. 5 Powder X-ray diffraction pattern of DMSI

Fig. 6 NMR Spectrum

Fig. 7 Optical absorption spectrum of DMSI

Fig. 8a TG/DTG Spectrum of DMSI crystal

Fig. 8b DSC Spectrum of DMSI crystal

Fig. 9 Impedance spectrum of DMSI crystal

Fig. 10a Variation of hardness with load

Fig. 10b Plot of log P Vs log

Table Caption

Table 1. Single crystal XRD data of DMSI

Table 2. CHN data

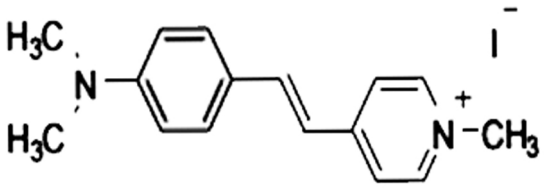

Fig. 1 Molecular structure of DMSI

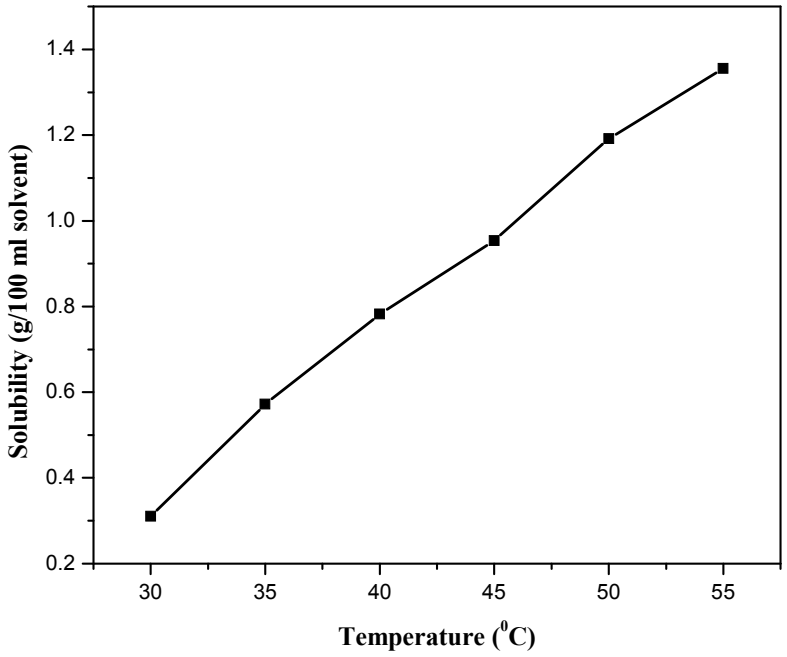

Fig. 2 Solubility curve of DMSI

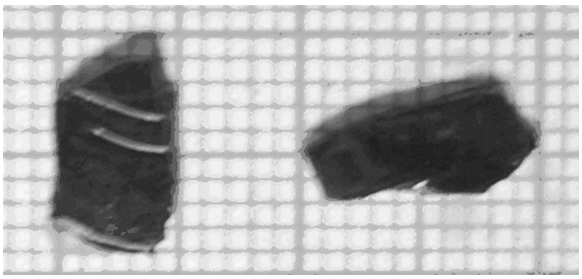

Fig. 3 Photograph of DMSI crystals

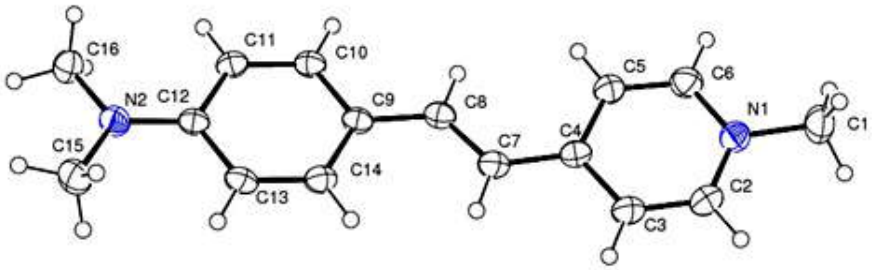

Fig. 4 Ortep diagram of DMSI single crystal

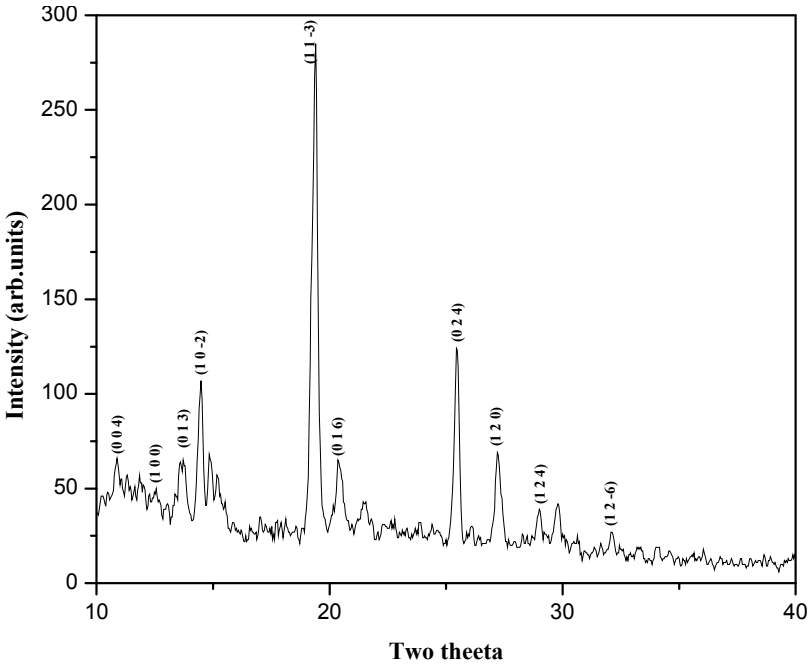

Fig. 5 Powder X-ray diffraction pattern of DMSI

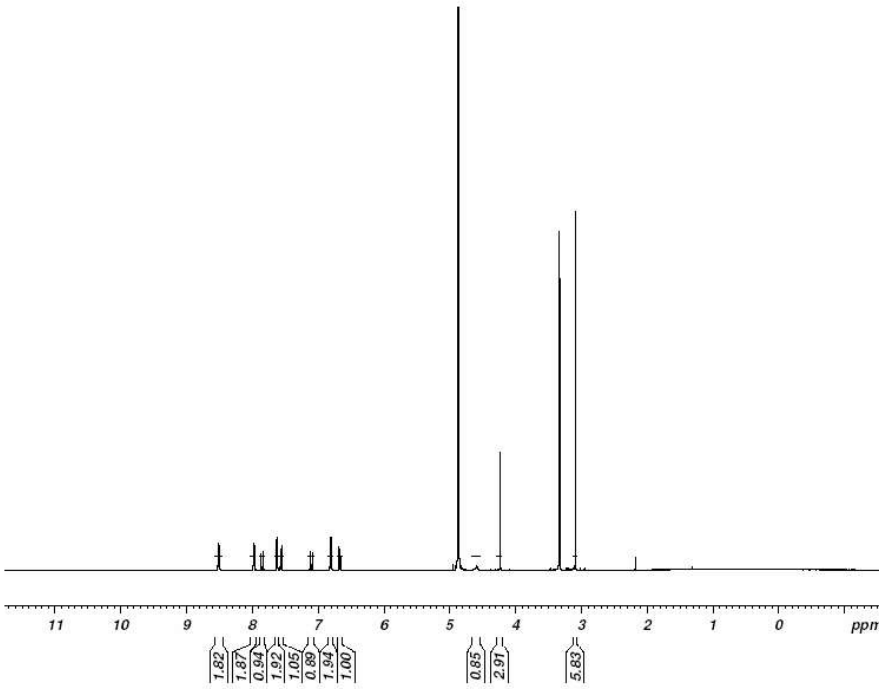

Fig. 6 NMR Spectrum of DMSI

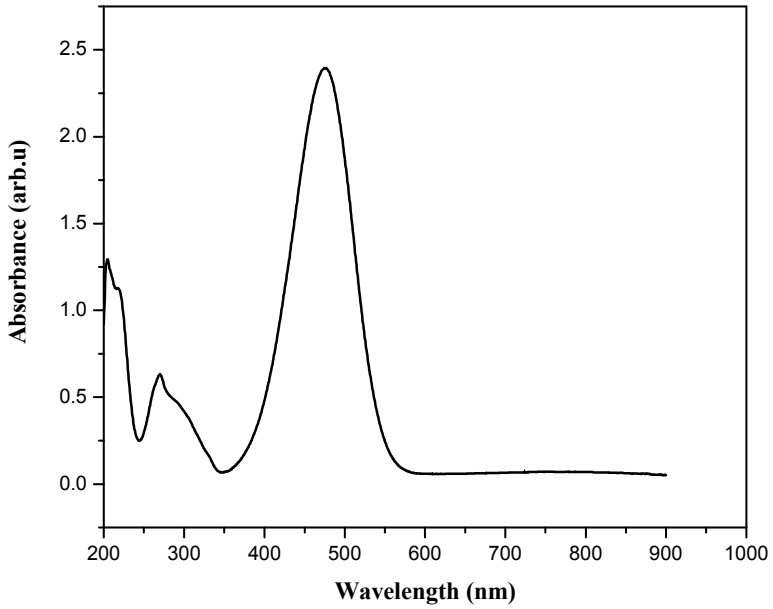

Fig. 7 Optical absorption spectrum of DMSI

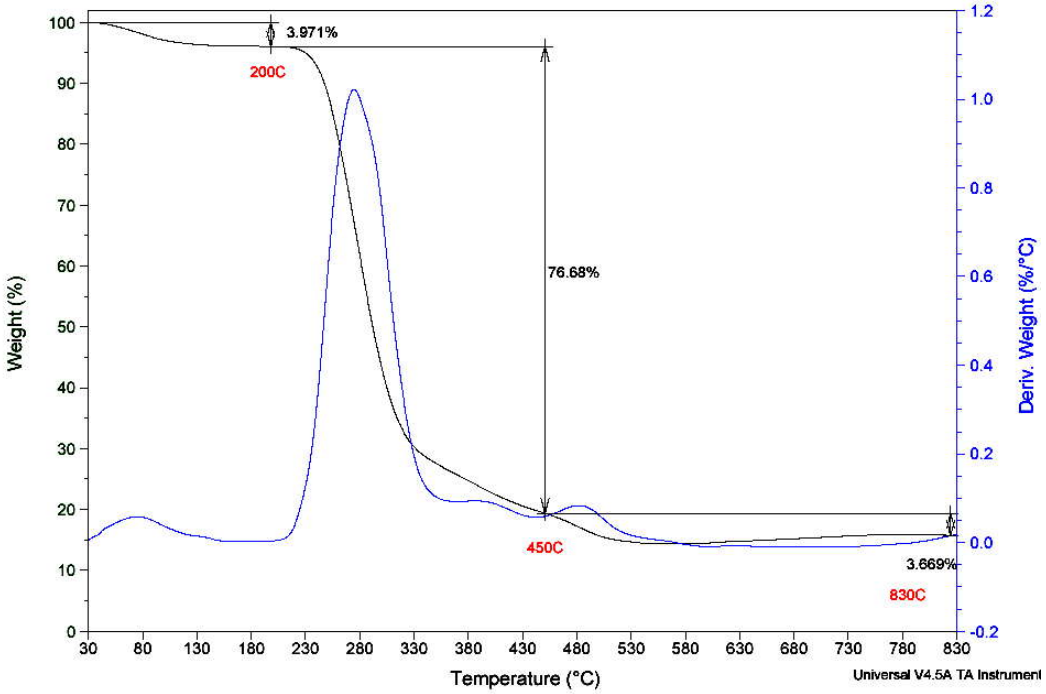

Fig. 8a TG/DTG Spectrum of DMSI

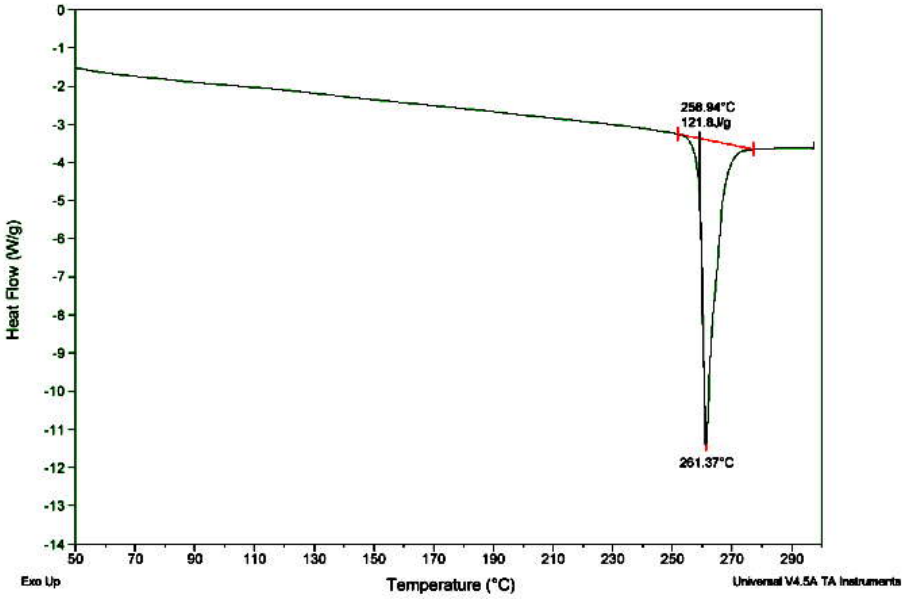

Fig. 8b DSC Spectrum of DMSI

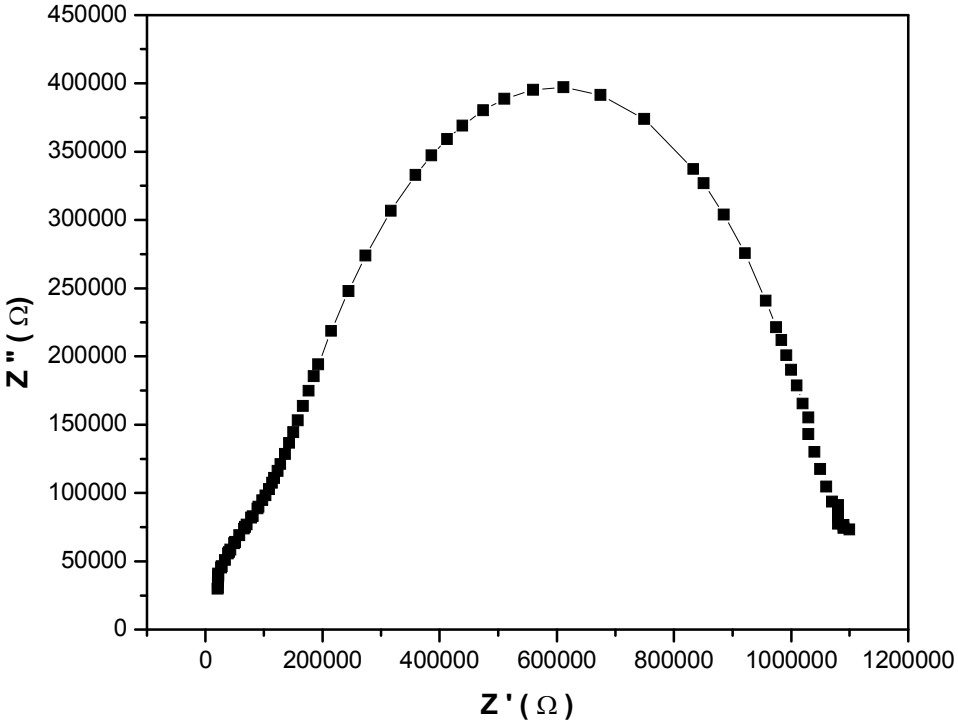

Fig. 9 Impedance spectrum of DMSI crystal

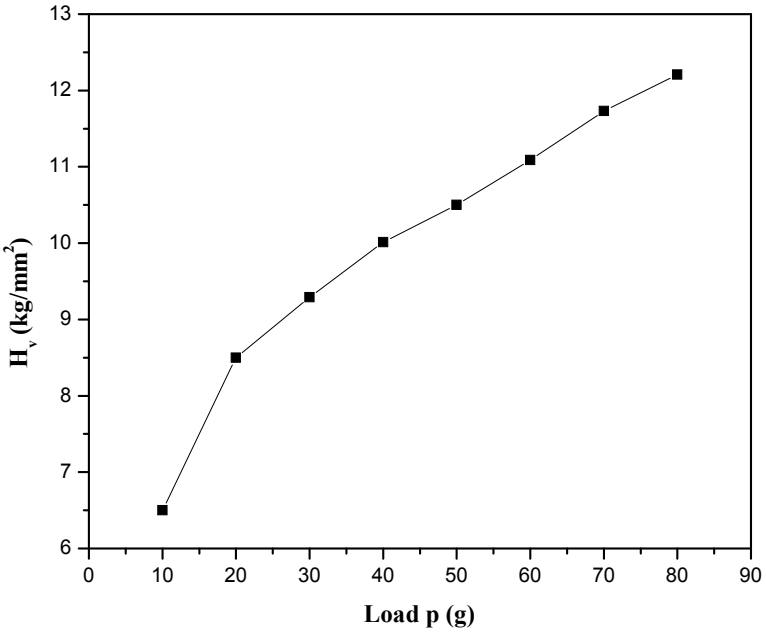

Fig. 10a Variation of hardness with load

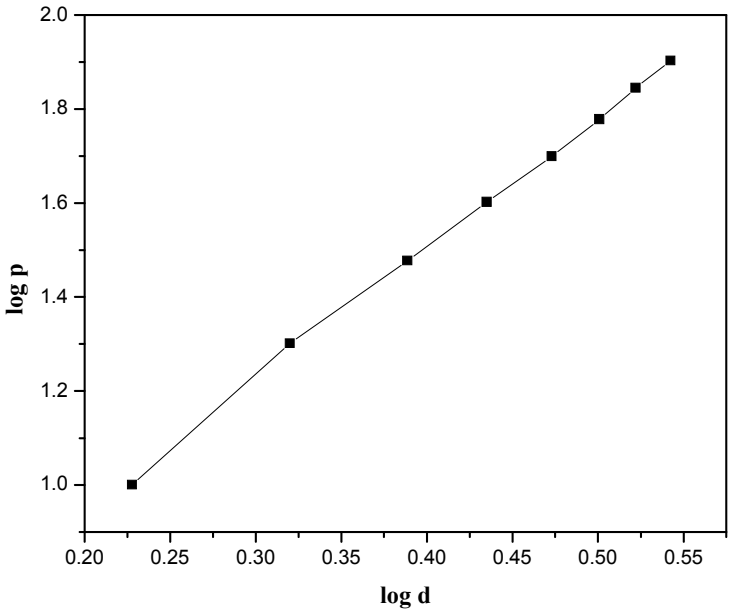

Fig. 10b Plot of log P Vs log d

Table 1 Single crystal XRD data of DMSI

Empirical Formula	$C_{16}\ H_{19}\ I\ N_2$
Formula weight	366.23
Crystal system	Monoclinic
Space group	*P*21/*c*
a (Å)	a = 6.3036(2)
b (Å)	b = 7.6547(2)
c (Å)	c = 32.0095(9)
α	90 ^{o}
β	90.3150(10) ^{o}
γ	90 ^{o}
Volume ($Å^3$)	1544.50(8)
Molecules per unit cell (Z)	4
Calculated density (Mg/m^3)	1.575
Absorption coefficient (mm^{-1})	2.063

Table 2 CHN Data

DMSI	Calculated	Experimental
Formula	C_{16} H_{19} I N_2	C_{16} H_{19} I N_2
C %	80.29	80.46
H %	8	8.13
N %	11.7	11.25